The Behavior of Planetary Wave 2 in Preconditioned Zonal Flows

WALTER A. ROBINSON

Department of Atmospheric Sciences, University of Washington, Seattle, WA 98195

(Manuscript received 19 March 1986, in final form 14 July 1986)

ABSTRACT

The response of linear planetary wave 2 to changes in the isentropic zonally symmetric distribution of potential vorticity (PV) is investigated numerically. Wave 2 is sensitive to the width and position of a region where the meridional derivative of PV is weak, denoted the "surf zone", in the middle stratosphere. A narrow surf zone leads to an amplification of wave 2, and confines some of its Eliassen–Palm wave activity in high latitudes. For wider surf zones the wave activity is concentrated near the associated critical surface, and the amplitude of the wave decreases. Large changes in the wave amplitude and in the distribution of its activity are associated with the subtle changes in the zonal winds produced by modest modifications in the distribution of PV.

Basic states that include regions of reversed meridional gradients of PV lead to wave overreflection and strong poleward focusing of wave activity. The amplitude of wave 2 is enhanced in the presence of negative gradients, with large responses occurring for eastward traveling waves.

1. Introduction

A stratospheric sudden warming is unlikely to occur when increased wave forcing is applied to a climatological wintertime zonal flow (McIntyre, 1982). Typically, if a transient wave event is to destroy the polar vortex, the flow must have already been modified by previous Canadian and minor warmings. The importance of this "preconditioning" of the stratospheric flow has been demonstrated by Butchart et al. (1982) in a numerical simulation of the February, 1979 sudden warming, and is consistent with observations (Schoeberl, 1978) that warmings are typically preceded by episodes of enhanced planetary wave activity, distinct from the event that destroys the vortex.

Recent analyses of the isentropic distribution of potential vorticity (PV) in the middle stratosphere (McIntyre and Palmer, 1984; Butchart and Remsberg, 1986; Clough et al., 1985; Dunkerton and Delisi, 1986) suggested that preconditioning occurs when PV is irreversibly mixed by breaking planetary waves, although the relative importance of conservative mixing and diabatic processes in such events remains controversial. If PV is conserved on the time scale of planetary wave breaking, then a breaking wave should mix PV within the breaking region or "surf zone", and should leave behind a band of enhanced horizontal gradients of PV at the edge of a smaller polar vortex.

McIntyre (1982) proposed two mechanisms by which preconditioning promotes the occurrence of a sudden warming. First, a smaller polar vortex is more readily destroyed by a transient planetary wave. This requires large meridional displacements of parcels and is therefore a nonlinear effect. Second, the rearrangement of potential vorticity during preconditioning leads to a basic state which may focus wave activity from subsequent wave events into the vortex. This sensitivity of the waves to the basic state is potentially a linear effect, and has been studied in both models and the atmosphere using linear wave diagnostics (Palmer, 1981; Dunkerton et al., 1981). These investigations revealed that the planetary wave Eliassen–Palm (EP) flux penetrates into the polar regions in preconditioned flows, rather than refracting equatorward in the lower stratosphere as occurs in climatological flows. Some authors (Butchart et al., 1982; O'Neill and Youngblut, 1982; Kanzawa, 1982) have associated the focusing of wave activity with the structure of the planetary wave index of refraction.

In the present study we consider the linear aspects of the wave-breaking/wave-focusing process. The structure of linear planetary wave 2 is determined for a variety of zonal flows, defined by the isentropic zonally symmetric distribution of PV. Different basic states are constructed by rearranging PV in a fashion consistent with current ideas of wave breaking, and then solving the inversion problem to find the winds and temperatures.

In light of the many studies of linear planetary waves in the literature (Matsuno, 1970; Schoeberl and Geller, 1977; Lin, 1982; Jaqmin and Lindzen, 1985), it is important to emphasize what is different in the present work. Here basic states are constructed in a dynamically meaningful way. Flows that differ only by the redistribution of PV on isentropic surfaces are plausible states of the same conservative atmosphere at different times. More importantly, in defining basic states by their distributions of PV, we are specifying the distribution of

that dynamical quantity whose meridional derivative is essential to the existence of Rossby waves. This approach is justified a posteriori in that qualitatively similar wind profiles with different distributions of PV are found to support markedly different wave behavior.

There are a few drawbacks to this approach. We assume a very simple form for the rearrangement of PV, and wave breaking, in concert with nonconservative effects, may redistribute potential vorticity in a different way. The structure of the zonal mean PV can be modified by meridional circulations and interactions with gravity waves. Also, the assumption of a zonally symmetric basic state is not consistent with observations. Implicit in the assumption of zonal symmetry is the working hypothesis that it is the potential vorticity structure of the vortex, and not its location on or off the pole, that is important for the behavior of waves shorter than wave 1. Experiments with a more complicated model are needed to test this idea.

In the next section the procedure for finding winds and temperatures by inverting profiles of PV is described. The linear wave model is described in section 3. Section 4 contains the results of experiments in which wave 2 propagates through profiles with surf zones of varying width and position, and in section 5 basic states with regions of negative meridional gradients of PV are considered, as well as the behavior of traveling waves. A summary of the results and concluding remarks are in section 6.

2. Inversion of PV profiles

A prescription for inverting profiles of PV is presented in a recent paper by Hoskins et al. (1985). They explained that in order to carry out the inversion, balance conditions must be specified for the resulting flow. In the case of steady zonally symmetric flow the appropriate balance conditions are hydrostatic equilibrium and gradient wind balance. The inversion problem is nearly identical to Eq. (29) of their paper (note that the present notation is different from theirs),

$$\beta+\frac{1}{a}\frac{\partial\zeta}{\partial\phi}+Q\frac{\partial}{\partial\theta}\left(\frac{f_{\rm loc}}{R}\frac{\partial u}{\partial\theta}\right)=\frac{\sigma}{a}\frac{\partial Q}{\partial\phi} \tag{1}$$

where ζ is the zonal mean relative vorticity, β the meridional derivative of the planetary vorticity, u the zonal mean wind, a the radius of the earth, θ the potential temperature, and ϕ the latitude; Q is the potential vorticity given by

$$Q=(f+\zeta)/\sigma \tag{2}$$

where f is the coriolis parameter and σ is the static stability

$$\sigma=-\frac{\partial P}{\partial\theta}, \tag{3}$$

P is the pressure, $f_{\rm loc}$ is the "local coriolis parameter" given by

$$f_{\rm loc}=f+\frac{2u}{a}\tan\phi \tag{4}$$

and R is a function of P,

$$R=\kappa\frac{\pi}{P} \tag{5}$$

where π is the Exner function

$$\pi=c_p\left(\frac{P}{P_0}\right)^{\kappa}; \tag{6}$$

κ is the ratio of the gas constant of air to its specific heat at constant pressure, c_p.

The balance condition,

$$f_{\rm loc}\frac{\partial u}{\partial\theta}=\frac{-1}{a}\frac{\partial\pi}{\partial\phi} \tag{7}$$

is applied to find values of R and σ in Eq. (1) that are consistent with the zonal wind field. If u is known, Eq. (7) can be integrated over latitude to obtain π and thus P as a function of potential temperature and latitude. The constant of integration is determined by fixing the globally integrated isentropic distribution of mass,

$$\int P(\theta,\phi)\cos\phi d\phi=P_{\rm ref}(\theta)\int\cos\phi d\phi \tag{8}$$

where $P_{\rm ref}$ is the mean pressure of an isentropic surface.

Equation (1) is an elliptic partial differential equation for u, and can be solved, using second-order finite differences on a $\ln\theta$–latitude grid, by successive overrelaxation. To correct P, R and σ, a Simpson's rule integration of Eq. (7) is performed after every n iterations on Eq. (1). In practice, fastest convergence is found for $n\sim 10$. The constant of integration is determined by a Newton-Rapheson iteration of the condition (8); $f_{\rm loc}$ is updated at each iteration using the values of u from the previous step. The iteration is stopped when the largest residual at any gridpoint is less than $0.002\times\Omega/a$.

In the present application there is some arbitrariness in the choice of boundary conditions for Eq. (1). For reasons of computational efficiency, the inversion and subsequent wave modeling are performed in a hemispheric domain. The meridional gradient of u is taken to vanish at the equatorial boundary. This gives more realistic zonal winds than forcing $u=0$ at the equator. At the pole, $u=0$.

The most unphysical condition is applied at the top of the domain. Fortunately, winds more than a scale height below the top are insensitive to exactly how the top is treated. The smoothest profiles are produced when the inversion is carried out at the top row of grid points under the assumption that the winds there have no curvature in $\ln\theta$. On the lowest isentrope the winds are held fixed at realistic lower tropospheric values. This is a reasonable procedure only in the present ap-

plication in which the rearrangement of PV is confined to the stratosphere.

The linear wave model, described in the next section, uses a log–pressure vertical grid, so winds must be interpolated to this grid after the PV inversion is complete. The full procedure is as follows: A realistic wintertime zonal wind profile is defined on the $\ln P$–latitude grid. The temperature profile at the equator is also specified, allowing the temperature, potential temperature and potential vorticity to be determined at every pressure and latitude by numerical integration of the thermal wind equation and subsequent finite differencing of the winds and potential temperatures. The potential vorticity is interpolated to a $\ln\theta$ grid using cubic splines.

After the PV is rearranged and the inversion is performed as described above, the resulting winds are interpolated back to the $\ln P$ grid using cubic splines, and values of $\ln\theta$ at every point are found by linear interpolation. To insure that the final zonal flow in the $\ln P$ coordinate is in gradient wind balance, the interpolated temperatures are used only on the equator. Elsewhere temperatures are found by meridional integration of the thermal wind equation.

3. Linear wave model

The model used in this study is derived from that developed by Hendon and Hartmann (1982). The present model differs from theirs in that the zonal winds are taken to be in gradient, as opposed to geostrophic, balance, the static stability varies with both pressure and latitude, and a log–pressure vertical coordinate is used. The model domain is the Northern Hemisphere, from the surface to 0.1 mb. There are 24 levels and 37 meridional grid points.

Planetary wave 2 is forced by vertical velocities corresponding to flow over a Gaussian distribution of orography, centered on 55°N with a width of 15 degrees. The results discussed below are insensitive to the latitude and width of the forcing. Wave geopotential is constrained to vanish at the equator, and there is a rigid lid at the top of the model. Spurious reflections from the top and equatorial boundaries are prevented by a sponge layer of equal rates of Newtonian cooling and Rayleigh friction confined to within 5 km of the lid and 5 degrees of the equatorial boundary. The damping rates at the boundaries are 10^{-5} s^{-1}, and they decay smoothly to zero in the interior of the domain. The results in the interior are unaffected when the sponges are removed, but the values of some wave quantities become noisy near the boundaries. Results from a global model with no equatorial boundary are essentially identical to those obtained with the hemispheric model including the sponge layer.

Away from the boundaries there is no dissipation in the model. Instead waves are forced with a complex frequency corresponding to constant exponential growth of the wave. In a steady model the imaginary part of the frequency is equivalent to constant equal rates of Newtonian cooling and Rayleigh friction. For our present purposes, this offers some advantages over more realistic parameterizations of dissipation. First, it is reasonable to consider growing waves in studying the initial behavior of disturbances that cause sudden warmings. Such waves are presumably growing during that period for which linear theory is applicable. Second, using a constant growth rate allows a particularly simple interpretation of the divergence of the EP flux. For a wave with amplitude proportional to $\exp(\alpha t)$ and in the absence of dissipation, the equation for the density of Eliassen–Palm wave activity becomes

$$2\alpha A + \nabla \cdot \mathbf{F} = 0 \tag{9}$$

where A is the density of wave activity and $\mathbf{F}$ is the EP flux vector. Plots of EP flux divergence are also plots of wave activity density.

The results are rather insensitive to the growth rate (or equivalently rate of dissipation) employed. For smaller growth rates the wave is more sensitive to changes in the zonal flow, and for growth rates an order of magnitude smaller the wave "feels" the boundaries. Similarly, the wave becomes more confined in high latitudes and less sensitive to the structure of the zonal flow as the growth rate is increased. Experiments with steady waves using realistic values of Newtonian cooling and Rayleigh friction produced results similar to those discussed below.

4. Results with surf zones of varying width

In what follows we are primarily concerned with the effects on planetary waves of the strength and location of a region of weak or reversed meridional gradients of PV, denoted the surf zone. We take as an initial basic state the zonal wind profile shown in Fig. 1a. These winds are similar to the January profile shown by Geller et al. (1983). The isentropic gradients of PV associated with these winds are shown in Fig. 1b. In these and other figures showing meridional gradients of PV, values are multiplied by the mean value of σ at that level, and are scaled by $2\Omega/a$. Thus, the values plotted represent the ratio of the isentropic gradient of PV to that at the equator in a motionless atmosphere with static stability equal to the average value at that height. This convention allows gradients of PV over a wide range of heights to be depicted in a single figure. The profile in Fig. 1 has strong gradients of PV in the tropospheric and stratospheric jets, with weaker gradients south of the stratospheric jet, but the gradients are substantially different from zero everywhere. Following Butchart and Remsberg (1986), the PV structure on the 850 K isentrope is presented by graphing the area contained within a PV contour against the value of the PV on that contour. In the present case this is simply a plot of the sine of latitude against the PV at

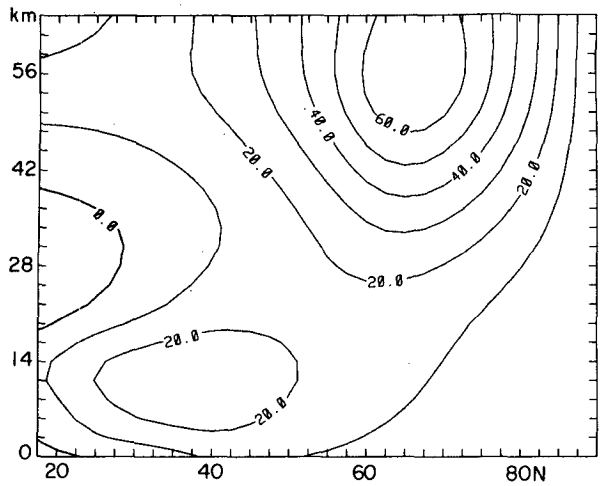

FIG. 1a. Zonal winds for a zonal flow with no surf zone. The contour interval is 10 m s^{-1}. The vertical axis is the log-pressure height computed assuming a scale height of 7 km.

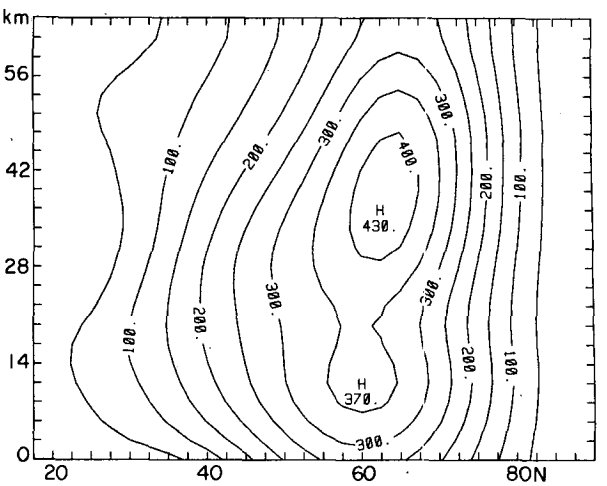

FIG. 2a. Geopotential amplitude of wave 2 in a flow with no surf zone. The contour interval is 50 m.

that latitude. The profile of Fig. 1 corresponds to curve A in Fig. 4. Note that any conservative isentropic rearrangement of PV leaves the area under such curves unaltered.

Figure 2a shows the geopotential amplitude of wave 2 in this zonal flow. The wave is forced by wave 2 topography with an (arbitrary) amplitude of 1000 m, and a growth rate of 2×10^{-6} s^{-1} is specified, corresponding to an *e*-folding time of about 6 days. The amplitude is largest in the lower portion of the stratospheric jet, and the hint of a node at 20 km suggests that vertical trapping is significant. This wave structure does not agree very well with observations (Geller et al., 1983; van Loon et al., 1973). Structures that show better agreement with observations are found when the zonal flow includes a surf zone (below).

Figure 2b shows the divergence of the EP flux, with dimensions of torque per unit mass. According to Eq. (9) this is also a plot of the density per unit mass of wave activity, a convergent EP flux corresponding to positive wave activity. Figures 2a and 2b are entirely dissimilar. Because Fig. 2b shows where the wave can interact strongly with the mean flow, from a dynamical standpoint it is a better picture of where wave 2 is "big". In this case the activity of wave 2 is concentrated at 30 km altitude in the weak westerlies north of the zero wind line. The maximum at the surface results from the combined effects of the weak winds there and the exponential growth of the wave.

Figure 3 shows the quasi-geostrophic index of refraction (Palmer, 1982) for wave 2. (This is the only

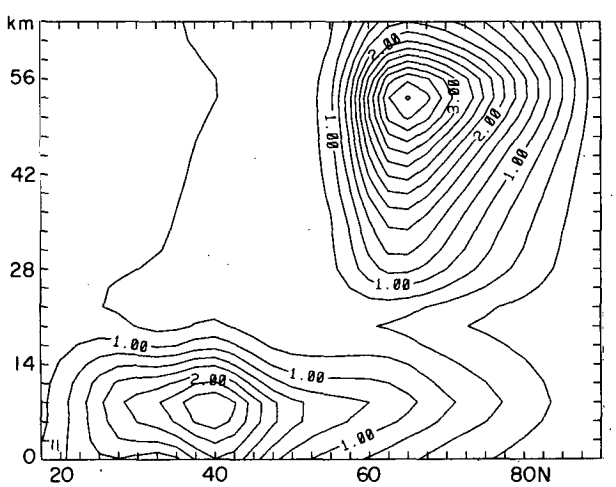

FIG. 1b. The scaled meridional derivative of potential vorticity for this flow (see text). The contour interval is 0.25.

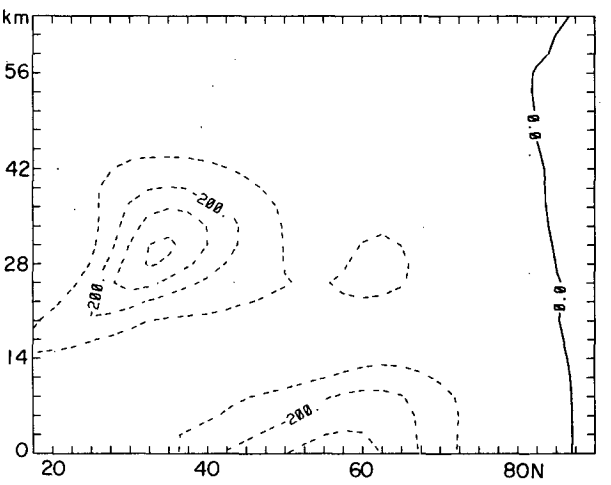

FIG. 2b. Divergence of the Eliassen–Palm flux for this wave. Negative values are indicated by dashed contours, and the contour interval is 100 m^2 s^{-2}. Negative values correspond to a positive density of wave activity.

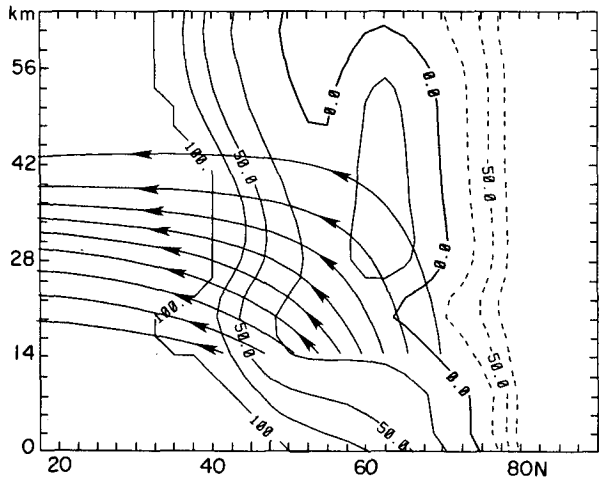

FIG. 3. Integral curves of the Eliassen–Palm flux (solid curves with arrows) superimposed on the quasi-geostrophic squared index of refraction for wave 2 in a flow with no surf zone. Contours are drawn every 25 units, and dashed contours represent negative values. No contours are shown for values greater than 100 or less than −100.

quasi-geostrophic quantity presented; primitive equation forms are used for the EP flux and its divergence.) Superimposed on the contours of refractive index are integral curves of the EP flux, curves that are everywhere parallel to the EP flux vector. The curves start at the 136-mb level. The leftmost curve starts at a point such that one-tenth of the upward EP flux across this level enters the stratosphere between this point and the equator. One-fifth of the upward flux enters the stratosphere between the beginning of the second curve and the equator, and so on. In this case there is no significant flux of wave activity into the polar stratosphere. Under the quasi-geostrophic approximation, ray tracing theory predicts that the EP flux should be refracted up the gradient of the index of refraction. While the curves do bend equatorward in response to the planetary scale southward increase in the index, the EP flux is insensitive to smaller scale variations. The curves show no tendency to follow the weak ridge in the index associated with the stratospheric jet.

The profile of Fig. 1 is modified by inserting a region of weak meridional gradients of PV. The meridional structure of the new PV distribution is given by

$$Q = \exp\left[-\frac{(y-y_s)^2}{w}\right] \times (Q_{ys}(y-y_s) + Q_0(y_s) - Q_0(y)) + Q_0(y) \quad (10)$$

where y is the sine of latitude, y_s the value of y at the center of surf zone, w the width of the surf zone, $Q_0(y)$ the unmodified distribution of PV, and Q_{ys} the meridional gradient of PV imposed at the center of the surf zone. For the results described below, the PV profile is modified between 20 and 40 km altitude, with smooth transitions to the preexisting structure above and below. When $Q_{ys} = 0$, the modified structure has a region of flat Q, bracketed to the north and south by increased gradients. The width of the surf zone, w, is chosen such that the increased gradient north of the surf zone coincides with the southern edge of the jet, 60°N.

Curve "B" in Fig. 4 shows the PV structure on the 850 K isentrope with a surf zone centered on 40°N. The meridional gradients of PV are shown in Fig. 5b, and the associated zonal winds in Fig. 5a. Figures 1a and 5a are similar, the principal difference being the poleward extension of the tongue of easterlies in Fig. 5a. That reduced values of $dQ/d\phi$ are associated with easterlies or weakened westerlies is consistent with the idea that Eq. (1) is approximately a scaled Poisson equation for u, forced by $-dQ/d\phi$ (Hoskins et al., 1985). Figure 5a also shows a subtle sharpening of the westerlies in the lower portion of the jet, associated with the increase in $dQ/d\phi$ north of the surf zone.

Figure 6a shows the geopotential amplitude of wave 2 in this zonal flow. The amplitude in the jet is increased by 50 percent over that in Fig. 2a. The density of wave activity (Fig. 6b) increases throughout the depth of the jet. In addition, the principal maximum in the wave activity shifts northward, following the region of weak westerlies.

By considering the results for a third profile, we see that the increased wave activity in the jet is not a consequence of the northward displacement of the zero wind line. Figure 8 shows the activity of wave 2 in a zonal flow with a surf zone at 45°N (Fig. 7). The narrower surf zone leads to a smaller maximum geopotential amplitude, 588 m, than occurred with the surf zone at 40°N, but there is still a concentration of wave

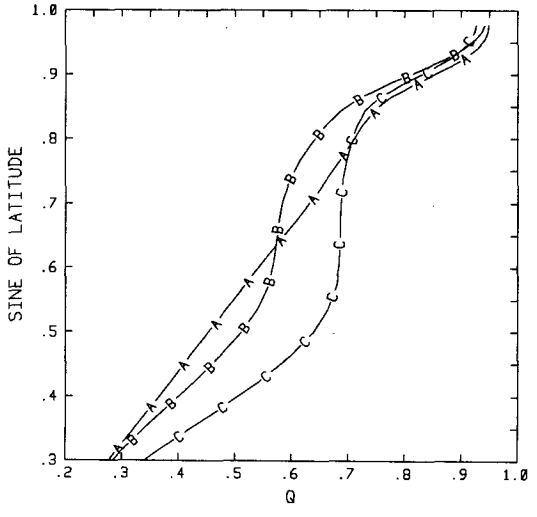

FIG. 4. Scaled potential vorticity plotted against the sine of latitude on the 850 K isentropic surface for a flow with no surf zone (curve A), flow with a surf zone at 40°N (curve B), and a flow with an asymmetric surf zone at 40°N (curve C).

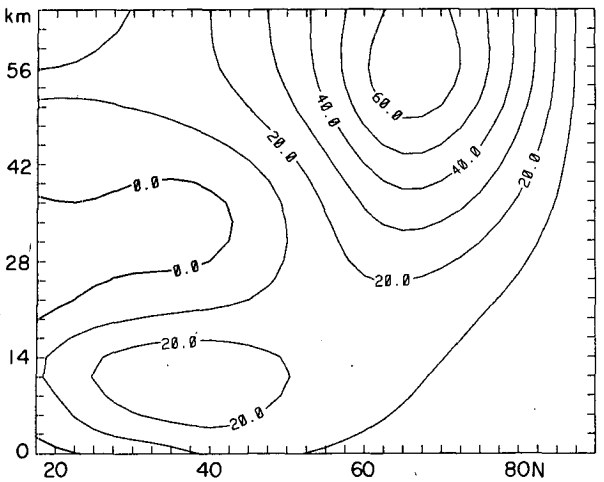

FIG. 5a. As in Fig. 1a but for a flow with a surf zone at 40°N.

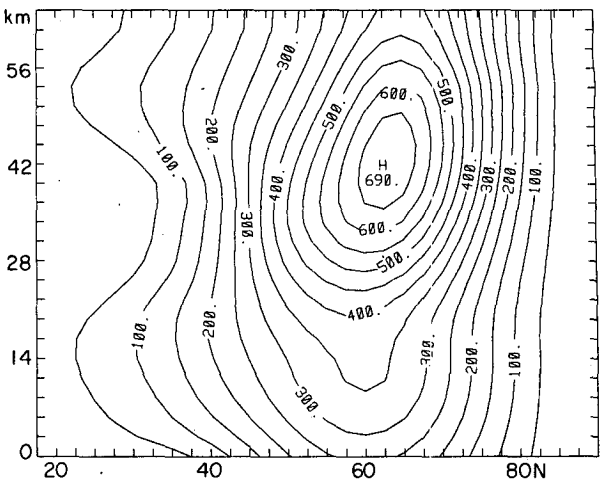

FIG. 6a. As in Fig. 2a but in a flow with a surf zone at 40°N.

activity in the jet that is clearly separated from the subtropical maximum associated with the zero wind line.

Figure 9 shows the index of refraction and integral curves of the EP flux for the flow with its surf zone at 45°N. The EP flux appears to flow undisturbed across the small region of negative refractive index associated with the surf zone. The meridional extent of this region is much smaller than the meridional wavelength of wave 2, so the slowly varying mean flow assumption needed for ray tracing is severely violated. Rather than the preconditioned zonal flow focusing the wave by smoothly refracting rays into high latitudes, it appears that the wave is partially reflected by the surf zone. Thus, large differences in the wave amplitude and the distribution of wave activity among Figs. 2, 6 and 8 are not reflected in the integral curves of the EP flux (Figs. 3 and 9). The idea that a region of weak meridional gradients of potential vorticity can partially trap waves in high latitudes was introduced by Matsuno (1970), who referred to the "cavity-like structure" of the index of refraction.

In order to verify that the wave amplifies in response to partial reflection from the surf zone and is unaffected by the sharpening of the jet, a profile is constructed in which there is a surf zone, but $dQ/d\phi$ in the jet is unaltered. The PV structure for this zonal flow with an asymmetric surf zone is represented by curve "C" in Fig. 4, and the associated winds are shown in Fig. 10. Figure 11 shows the wave activity density for wave 2 in this zonal flow. The wave amplitude is very similar to that shown in Fig. 6a. While the distribution of wave activity appears to be quite different from that in Fig. 6b, closer examination reveals that within the stratospheric jet the structures are nearly identical. In low latitudes the strong westerlies associated with the

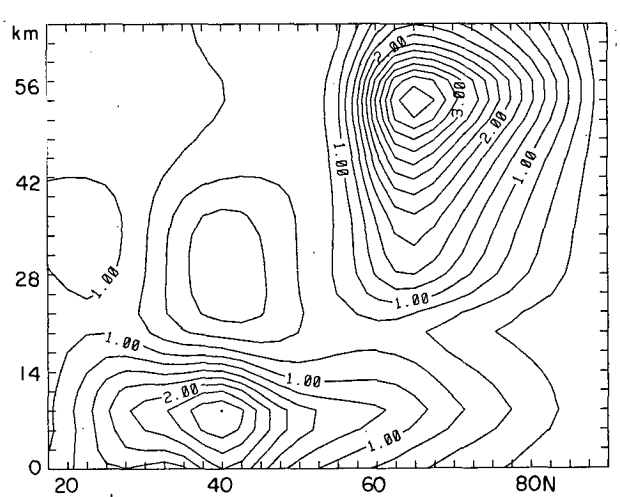

FIG. 5b. The scaled meridional derivative of PV for this flow.

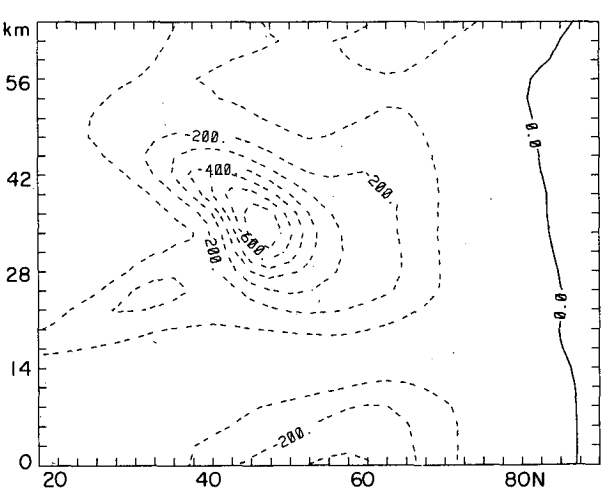

FIG. 6b. The divergence of the Eliassen–Palm flux for this wave.

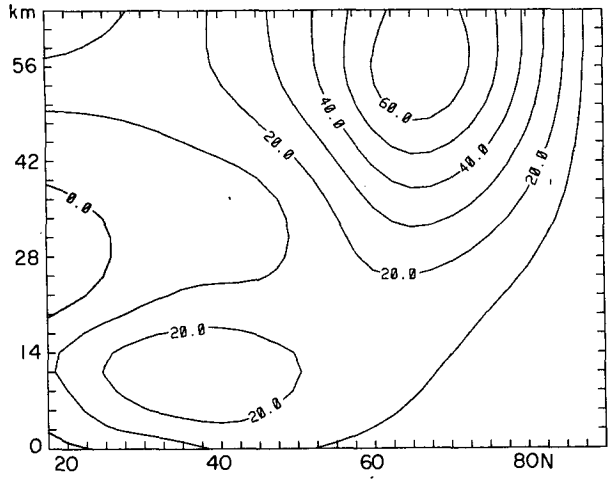

FIG. 7. As in Fig. 1a but for a flow with a surf zone at 45°N.

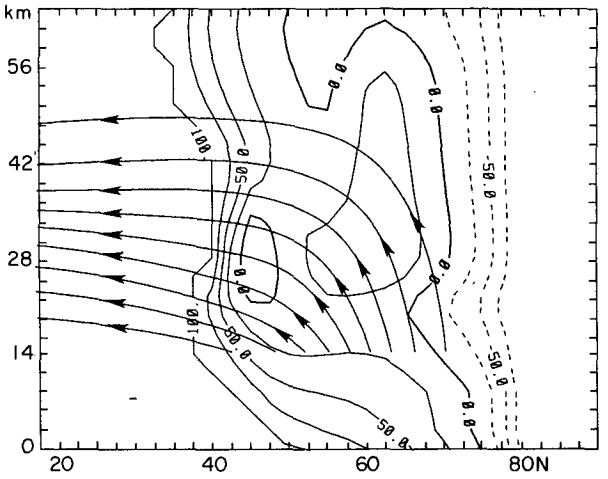

FIG. 9. As in Fig. 3 but for a flow with a surf zone at 45°N.

asymmetric surf zone permit some of the wave activity to reach the model's lid. However, the similarity in the region of the jet between the wave structures with symmetric and asymmetric surf zones confirms that it is the surf zone, and not a change in the structure of the jet, that is crucial to the differences between waves in the presence and in the absence of a surf zone.

When the center of the surf zone is moved equatorward from 40°N, and the surf zone is widened, the amplitude of wave 2 decreases. Figures 12 and 13 display the zonal flow and EP flux divergence of wave 2 for a surf zone centered at 30°N. The wave amplitude (maximum value of 372 m) is smaller than in the absence of a surf zone, and the distribution of wave activity has collapsed into the vicinity of the zero wind line, which now reaches to 45°N.

The increase in wave amplitude with the width of the surf zone, as seen from Figs. 2a and 6a, can be interpreted as the improved reflectivity of the low $dQ/d\phi$ region, in which Rossby waves are evanescent, as it is broadened. The decrease in wave amplitude as the surf zone is widened further can be understood in terms of the behavior of a linear Rossby wave critical layer. Linear theory predicts that the reflectivity of a critical layer increases as the potential vorticity gradient in the layer decreases (Tung, 1979). In the present experiments, as the surf zone is broadened, and the zero wind line shifts northward and into a region of stronger meridional gradients of PV (compare Fig. 5 and 12). The association between the width of the surf zone, and the value of $dQ/d\phi$ at the zero wind line is demonstrated for a simple barotropic flow in Appendix A. Broader surf zones are associated with more absorbing critical layers, explaining the decrease in wave amplitude for wider surf zones and the concentration of wave activity near the critical surface.

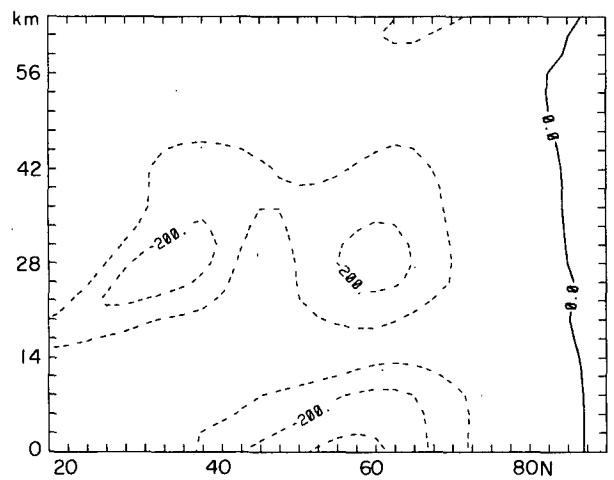

FIG. 8. The divergence of the Eliassen–Palm flux of wave 2 in a flow with a surf zone at 45°N.

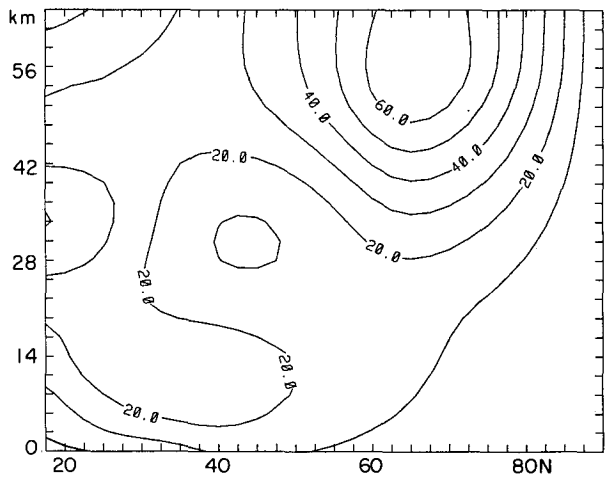

FIG. 10. As in Fig. 1a but for a flow with an asymmetric surf zone at 40°N.

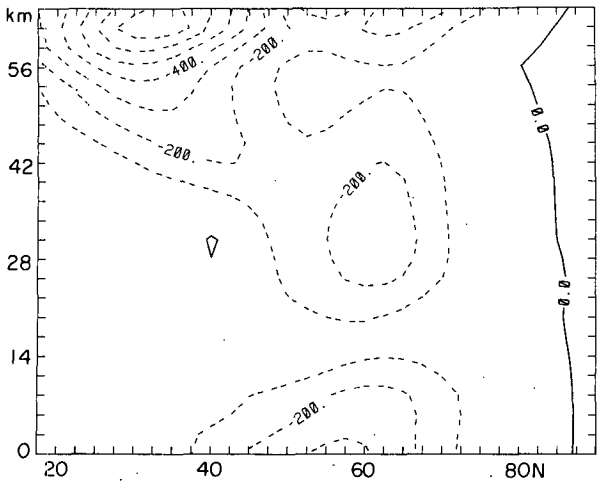

FIG. 11. The divergence of the Eliassen–Palm flux for wave 2 in a flow with an asymmetric surf zone at 40°N.

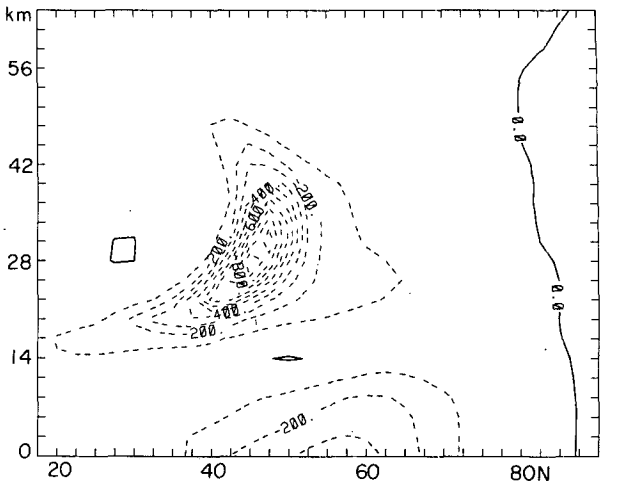

FIG. 13. The divergence of the Eliassen–Palm flux for wave 2 in a flow with a surf zone at 30°N.

5. Surf zones with reversed gradients of PV

Recent observational evidence suggests that preconditioning can lead to PV profiles with surf zones in which $dQ/d\phi$ is not merely weak, but is negative (Hitchman, 1985; Dunkerton and Delisi, 1986; Kanzawa, 1982). Such structures seem most likely to appear in the intermediate stages of a Rossby wave breaking event, after there has been considerable deformation of PV contours but before mixing to small scales has completely wiped out spatial gradients (P. Haynes, personal communication, 1986). Judging from stratospheric maps of PV, a negative meridional derivative of PV in the zonal mean would be an average over longitudes poleward of tongues of high PV air and longitudes where the PV decreases monotonically from the polar vortex to the tropics. Such tongues reaching into low latitudes are visible in results presented by Dunkerton and Delisi (1986), Clough et al. (1985) and McIntyre and Palmer (1984).

Figure 14 shows u for a flow with a weakly negative meridional derivative of PV in a surf zone at 45°N. These winds are similar to those shown in Fig. 7 for a flat surf zone, but the behavior of wave 2 in the two flows is very different. Figure 15 shows the wave activity of wave 2 in the flow depicted in Fig. 14. The amplitude of the wave (766 m) is much greater than when the surf zone is flat, and there is more wave activity in the region of the jet. The surf zone now supports a region of divergent EP fluxes or negative density of wave activity. The existence of this region is predicted by quasi-geostrophic theory. For a stationary wave growing exponentially with time, the quasi-geostrophic potential

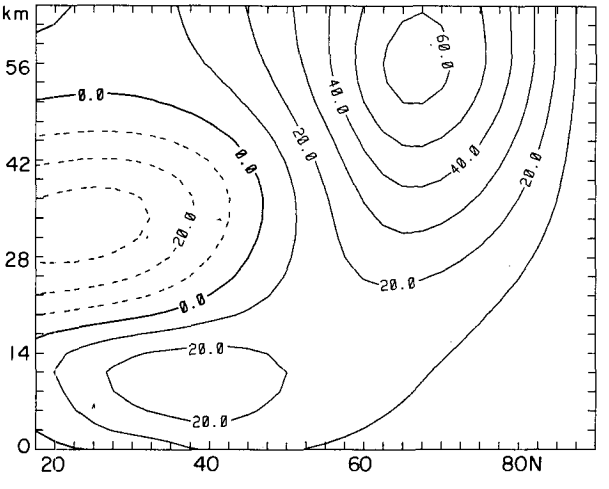

FIG. 12. As in Fig. 1a but for a flow with a surf zone at 30°N. Easterly winds are indicated by dashed contours.

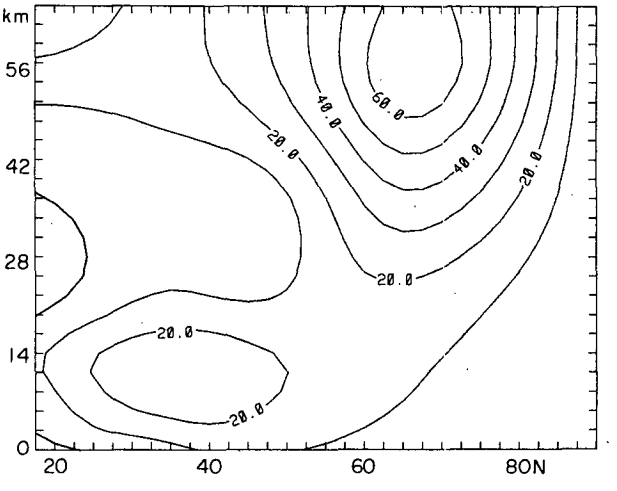

FIG. 14. As in Fig. 1a but for a flow with a surf zone with $dQ/d\phi < 0$ at 45°N.

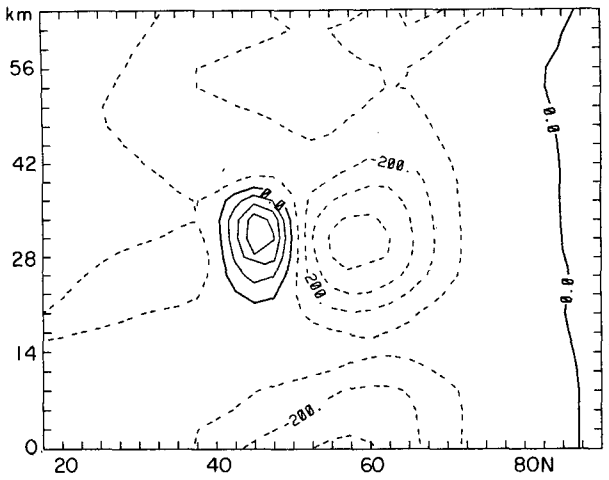

FIG. 15. The divergence of the Eliassen–Palm flux for wave 2 in the flow shown in Fig. 14.

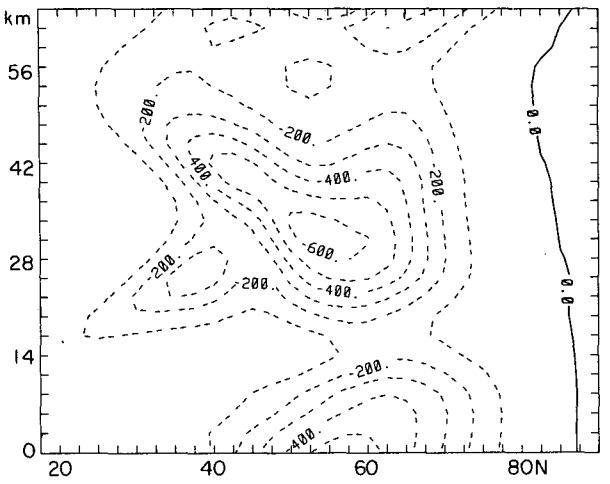

FIG. 17. The divergence of the Eliassen–Palm flux for wave 2 with an eastward frequency of 2.5 10^{-6} s^{-1} in a flow with a surf zone at 45°N.

enstrophy equation can be solved for the divergence of the EP flux:

$$\nabla \cdot \mathbf{F} = -2\alpha E/\bar{q}_y \qquad (11)$$

where α is the growth rate of the wave, E the potential enstrophy (a positive definite quantity), and $\bar{q}_y$ the meridional derivative of zonal mean potential vorticity. For a growing wave in a reversed gradient of potential vorticity, $\bar{q}_y < 0$, the EP flux is divergent.

Associated with the divergent EP flux is the exclusion from the surf zone of integral curves of the flux which originate lower in the atmosphere (Fig. 16), leading to stronger poleward focusing of wave activity than occurred in flows with flat surf zones. This difference (compare Fig. 9 and 16) may be relevant to observations of strong poleward focusing of wave activity preceding sudden warmings (Palmer, 1981). In experiments with a variety of zonal flows, only those with regions of $dQ/d\phi < 0$ exhibit the poleward deflection of curves of EP flux like that shown in Figs. 3b and 3c of Palmer's paper.

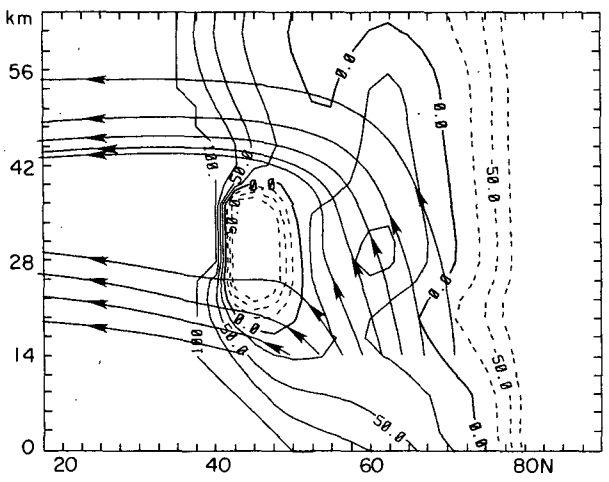

FIG. 16. As in Fig. 3 but for the zonal flow depicted in Fig. 14.

Numerical experiments performed by Butchart et al. (1982) indicated that the eastward progression of wave 2 was important in focusing the wave into high latitudes prior to the February 1979 major warming. Additional evidence for the eastward propagation of planetary waves during disturbed periods comes from observations of PV on stratospheric isentropes (Dunkerton and Delisi, 1986). When the polar vortex, defined as the region enclosed within a band of intense gradients of PV, is elongated, the elongated pattern tends to rotate counterclockwise. Since the elongation of the vortex is primarily associated with planetary wave 2, these observations support the eastward movement of wave 2.

In the present model, the behavior of a traveling wave can be investigated by adding a nonzero real component to the frequency of the wave. The magnitude of the vertical velocity that forces the wave from the bottom boundary is unchanged. Eastward traveling wave 2 with a frequency of 2.5 $\times$ 10^{-6} s^{-1} in a basic state without a surf zone has a larger amplitude (545 m) than a stationary wave in the same flow (Fig. 2), but its wave activity is still concentrated in the subtropics. The activity of the same wave traveling with the same frequency in a basic state which now includes a surf zone at 45°N is shown in Fig. 17. Its amplitude (867 m) and the extent to which the wave activity is confined to the region of the jet are enhanced in comparison both with a stationary wave in the same basic state (Fig. 8), and with a traveling wave in the absence of a surf zone.

The effects of the eastward phase speed are more pronounced when the surf zone includes reversed gradients of PV. Figure 18 shows the amplitude and den-

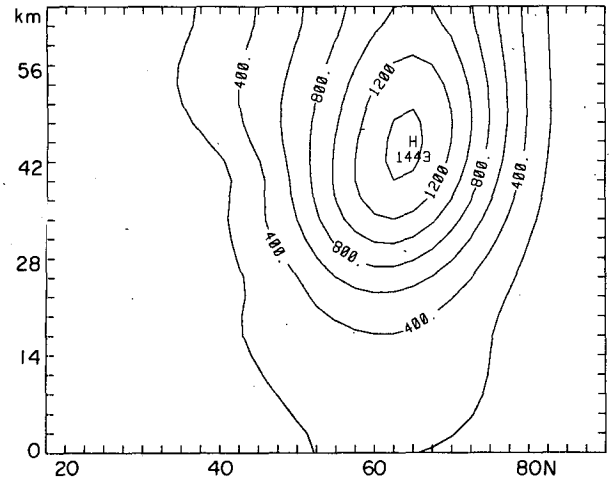

FIG. 18a. Eastward wave 2 in a flow with a surf zone with $dQ/d\phi < 0$ at 45°N. The contour interval is 200 m.

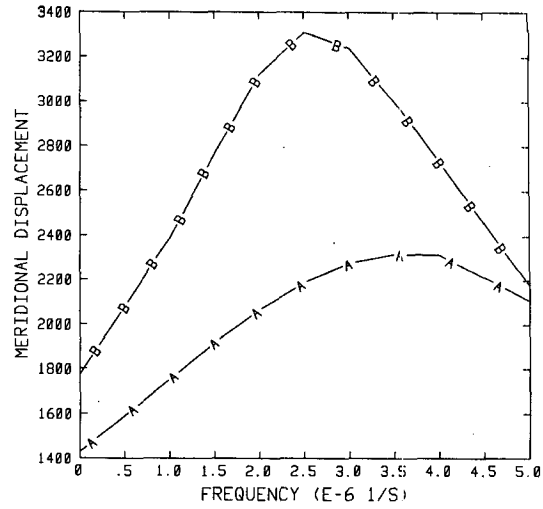

FIG. 19. Meridional displacement (km) of the PV contour at 60°N and 850 K as a function of the wave frequency in flow with a flat surf zone at 45°N (curve A), and with a surf zone with $dQ/d\phi < 0$ at 45°N (curve B).

sity of wave activity for wave 2 traveling eastward in the zonal flow of Fig. 14. The large wave amplitude and the high density of wave activity are striking. They suggest that the observed eastward propagation of wave 2 is a consequence of the selective linear amplification of eastward components of time-dependent tropospheric forcing.

To investigate this idea, the isentropic meridional displacement by the wave of a PV contour, $Q'(dQ/dy)^{-1}$, is computed for a range of wave frequencies in several basic states. The displacement of contours is what allows one to see the counterclockwise rotation of the vortex in a time series of PV maps. Figure 19 shows how the magnitude of the displacement of the PV contour at 60°N on the 850 K isentrope depends on frequency in basic states, with a flat surf zone at 45°N (curve A) and with $dQ/d\phi < 0$ at 45°N (curve B). The displacement is more sensitive to the frequency of the wave in the latter case, and the strongest response occurs at a frequency of 2.5×10^{-6} s^{-1}, corresponding to a phase velocity of 5.6 m s^{-1} at 45°N. The critical surface of this wave lies close to the surface of zero $dQ/d\phi$. That this should be the phase velocity at which the wave response is largest is consistent with theoretical expectations (Hoskins et al., 1985).

Figure 20 is similar to Fig. 19 but now the surf zones are centered at 40°N. Once again the wave is more sensitive to the frequency in the case with a reversed gradient of PV, but the strongest response is now at

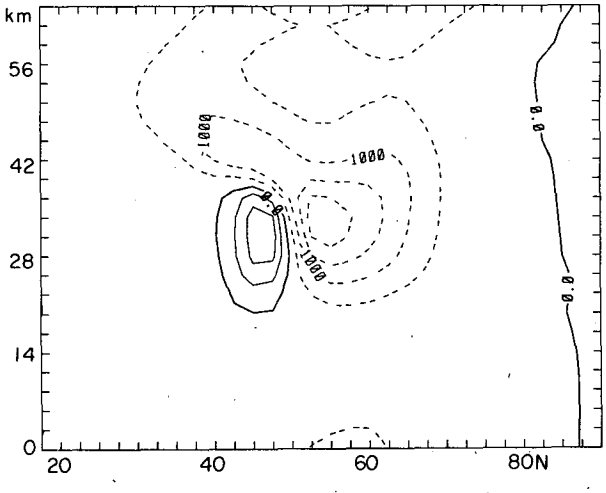

FIG. 18b. The divergence of the Eliassen–Palm flux for this wave. The contour interval is 500 m^2 s^{-2}.

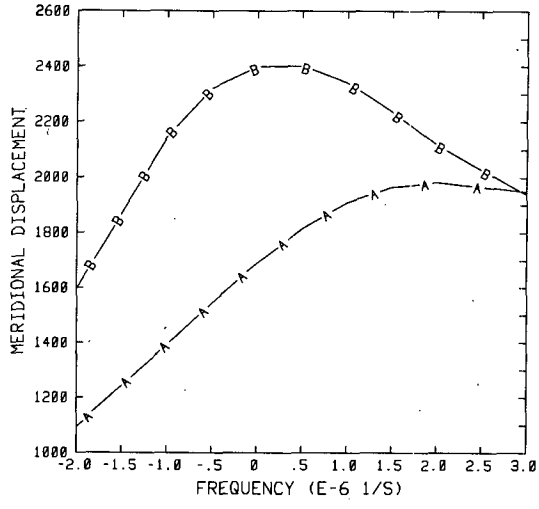

FIG. 20. As in Fig. 19 but with the surf zones centered at 40°N.

zero frequency. For this flow the zero wind surface lies nearby the boundary between regions of positive and negative $dQ/d\phi$.

6. Summary and discussion

The linear behavior of planetary wave 2 is calculated for a number of qualitatively similar zonal flows. Small changes in the zonal wind field induced by the isentropic rearrangement of PV result in significant changes in the structure of wave 2, especially in the distribution of its wave activity. These results confirm the fundamental importance of the potential vorticity as the dynamical quantity that determines the behavior of Rossby waves.

Specifically, a narrow region with a flat meridional distribution of PV, denoted a surf zone, tends to trap wave activity in higher latitudes, causing larger wave amplitudes at the base of the polar night jet. As the surf zone is expanded a growing region of easterlies appears at its center, as is expected from the quasi-Laplacian nature of the potential vorticity operator. The surface, $u = 0$, occurs in association with larger positive values of $dQ/d\phi$, resulting in increased critical layer absorption of stationary waves. So for narrow surf zones, the amplitude of wave 2 increases with the width of the surf zone, while for wider surf zones an increase in the width leads to a decrease in the amplitude of the wave. These results suggest that the extent to which the activity of a growing wave is confined to the region of the jet, and, therefore, the likelihood of a sudden warming may be sensitive to the details of how previous wave breaking events have rearranged PV.

The significance of these results depends on the relative importance of the structure of the stratospheric flow and the strength of tropospheric wave forcing in determining the flux of wave activity into the polar night jet. While we have shown that the former effect is not negligible, changes in the tropospheric forcing of the wave, the mechanisms for which lie beyond the realm of the present study, are probably essential. Presumably sufficiently strong wave forcing can induce a sudden warming in an unpreconditioned stratospheric flow. This is indeed what happens in quasi-linear mechanistic models in which a sustained wave event both preconditions the flow and causes the sudden warming.

It has been suggested that the focusing of wave activity into high latitudes is similar to the reflecting and overreflecting behavior of barotropic Rossby wave critical layers subjected to constant small wave forcing (McIntyre, 1982; Dunkerton et al., 1981). In the barotropic model the transition from absorption to reflection and overreflection, which is perhaps analogous to the preconditioning of the stratospheric flow, is accomplished by a single breaking wave. In the stratosphere, observations indicate that a sudden warming requires a sequence of wave events. The wave that destroys the vortex, causing the warming, encounters a flow that has been modified so that wave activity is reflected or overreflected from the subtropics into high latitudes.

In the present model the overreflecting state can only be represented by a zonally symmetric region in which the meridional gradient of PV is reversed. Such a flow supports a strong focusing of wave activity into high latitudes, similar to that observed prior to sudden warmings. The overreflecting surf zone also causes wave 2 to be sensitive to small changes in its zonal phase velocity. The wave response is largest when its critical surface lies near the surface of vanishing $dQ/d\phi$. In flows for which the surf zone is devoid of easterlies, such as that preceding the February 1979 major warming (Palmer, 1981), the basic state selectively reinforces eastward traveling waves. This is a possible explanation for the counterclockwise rotation of the elongated vortex that is visible in time series of PV maps during some disturbed periods.

Quasi-geostrophic instability theory (Charney and Stern, 1962), indicates that a zonal flow with an overreflecting surf zone may be unstable. Similarly, the more complicated structure of the overreflecting Rossby wave critical layer supports barotropic instabilities (Killworth and McIntyre, 1985; Haynes, 1985). A remaining question is whether subsequent wave events, in situ instability or dissipation, is most effective in destroying the long tongues of high PV air seen in stratospheric maps.

Acknowledgments. D. Hartmann generously provided the computer code for the linear wave model. P. Haynes helped in adapting the model and offered many helpful comments. M. Hitchman suggested the relevance of profiles with reversed gradients of PV. Comments from P. Hess, S. Yoden, M. McIntyre and three anonymous reviewers helped the author improve the clarity of the manuscript. This research was supported by NASA Grant NAGW-662.

APPENDIX A

Dependence of dq/dy on the Width of the Surf Zone at the Critical Line

Consider zonal barotropic flow on a beta-plane. The (potential) vorticity is

$$q = \beta y - u_y. \tag{A1}$$

A family of vorticity profiles with surf zones of width, w, are defined by

$$q = y\left[1 - \exp\left(-\tfrac{1}{2}(y/w)^2\right)\right] \tag{A2}$$

where y is a nondimensional meridional coordinate

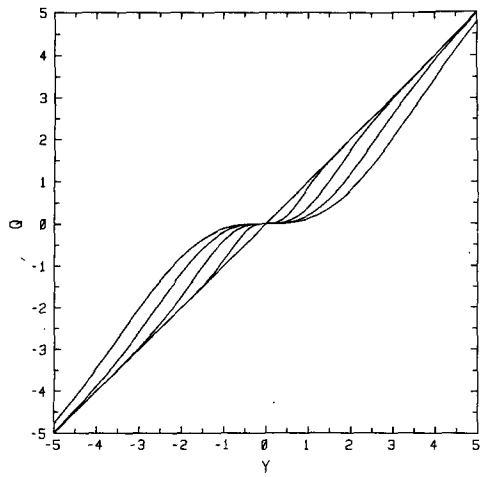

FIG. A1. Absolute vorticity for barotropic flows with surf zone widths of 0, ½, 1, ³⁄₂ and 2.

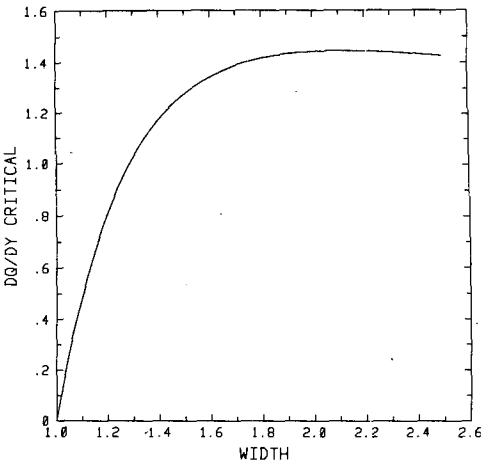

FIG. A3. Meridional derivative of the absolute vorticity at the zero wind line as a function of the surf zone width.

scaled by $(U/\beta)^{1/2}$ where U is the zonal wind velocity far from the surf zone, and q is scaled by $\beta(U/\beta)^{1/2}$. Substituting (A1) into (A2) and integrating, the nondimensional zonal wind is given by

$$u = 1 - w^2 \exp\left[-\frac{1}{2}(y/w)^2\right]. \tag{A3}$$

There is no zero wind line unless $w \geq 1$. Figure A1 shows profiles of q with $w = 0$, ½, 1, ³⁄₂ and 2. The associated winds are shown in Fig. A2.

The location of the zero wind line is given by

$$y = 2w(\ln w)^{1/2}. \tag{A4}$$

Differentiating A2 and substituting A4 gives the value of dq/dy at the stationary wave critical line (Fig. A3),

$$\left.\frac{\partial q}{\partial y}\right|_{u=0} = 1 - (1 - 4\ln w)/w^2. \tag{A5}$$

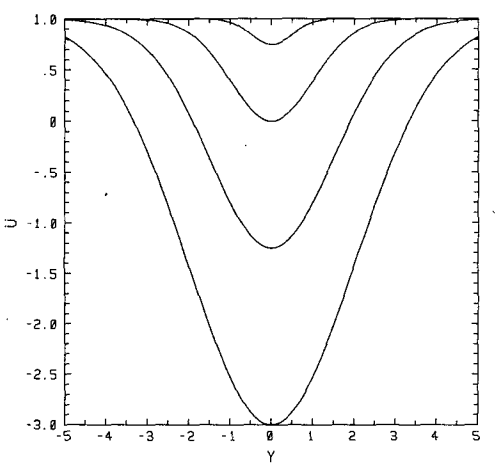

FIG. A2. Zonal winds associated with the vorticity profiles in Fig. A1.

In this simple case, for surf zone widths near to that at which easterly winds first appear, the vorticity gradient at the zero-wind line, and therefore the reflectivity of the linear critical layer for stationary waves, is sensitive to the width of the surf zone. For wide surf zones the critical line always lies in the region of enhanced vorticity gradients at edge of the surf zone.

REFERENCES

Butchart, N., and E. E. Remsberg, 1986: The area of the stratospheric polar vortex as a diagnostic for tracer transport on an isentropic surface. *J. Atmos. Sci.* (in press).

—— et al., 1982: Simulations of an observed stratospheric warming with quasigeostrophic refractive index as a model diagnostic. *Quart. J. R. Meteor. Soc.*, **108,** 475–502.

Charney, J. G., and M. E. Stern, 1962: On the stability of internal baroclinic jets in a rotating atmosphere. *J. Atmos. Sci.*, **19,** 159–172.

Clough, S. A., N. S. Grahame, and A. O'Neill, 1985: Potential vorticity in the stratosphere derived using data from satellites. *Quart. J. R. Meteor. Soc.*, **111,** 335–338.

Dunkerton, T. S., and D. P. Delisi, 1986: Evolution of potential vorticity in the winter stratosphere of January–February 1979. *J. Geophys. Res.*, **91,** 1199–1208.

——, C.-P. F. Hsu, and M. E. McIntyre, 1981: Some eulerian Lagrangian diagnostics for a model stratospheric warming. *J. Atmos. Sci.*, **38,** 819–843.

Geller, M. A., M.-F. Wu and M. E. Gelman, 1983: Troposphere–stratosphere (surface–55 km) monthly winter general circulation statistics for the Northern Hemisphere—four year averages. *J. Atmos. Sci.*, **40,** 1334–1352.

Haynes, P. H., 1985: Nonlinear instability of a Rossby-wave critical layer. *J. Fluid Mech.*, **161,** 493–511.

Hendon, H. H., and D. L. Hartmann, 1982: Stationary waves on a sphere: sensitivity to thermal feedback. *J. Atmos. Sci.*, **39,** 1906–1920.

Hitchman, M. H., 1985: An observational study of wave-mean flow interactions in the equatorial middle atmosphere. Ph.D. dissertation, University of Washington, pp. 374.

Hoskins, B. J., M. E. McIntyre and A. W. Robertson, 1985: On the use and significance of isentropic potential vorticity maps. *Quart. J. R. Met. Soc.*, **111,** 877–946.

Jacqmin, D., and R. S. Lindzen, 1985: The causation and sensitivity

of the northern winter planetary waves. *J. Atmos. Sci.*, **42,** 724–745.

Kanzawa, H., 1982: Elassen-Palm flux diagnostics and the effect of the mean wind on planetary wave propagation for an observed sudden stratospheric warming. *J. Meteor. Soc. Japan,* **60,** 1063–1072.

Killworth, P. D., and M. E. McIntyre, 1985: Do Rossby-wave critical layers absorb, reflect, or over-reflect? *J. Fluid Mech.*, **161,** 449–492.

Lin, B.-D., 1982: The behavior of winter stationary planetary waves forced by topography and diabatic heating. *J. Atmos. Sci.*, **39,** 1206–1226.

McIntyre, M. E., 1982: How well do we understand the dynamics of stratospheric warmings? *J. Meteor. Soc. Japan,* **60,** 37–65.

——, and T. N. Palmer, 1984: The "surf zone" in the stratosphere. *J. Atmos. Terr. Phys.*, **46,** 825–849.

Matsuno, T., 1970: Vertical propagation of stationary planetary waves in the winter Northern Hemisphere. *J. Atmos. Sci.*, **27,** 871–883.

O'Neill, A., and C. E. Youngblut, 1982: Stratospheric warmings diagnosed using the transformed Eulerian-mean equations and the effect of the mean state on wave propagation. *J. Atmos. Sci.*, 1370–1386.

Palmer, T. N., 1981: Diagnostic study of a wavenumber-2 stratospheric sudden warming in a transformed Eulerian-mean formalism. *J. Atmos. Sci.*, **38,** 844–855.

——, 1982: Properties of the Eliassen–Palm flux for planetary scale motions. *J. Atmos. Sci.*, **39,** 992–997.

Schoeberl, M. R., 1978: Stratospheric warmings: Observations and theory. *Rev. Geophys. Space Phys.*, **16,** 521–538.

——, and M. A. Geller, 1977: A calculation of the structure of stationary planetary waves in winter. *J. Atmos. Sci.*, **34,** 1235–1255.

Tung, K. K., 1979: A theory of stationary long waves. part III: quasi-normal modes in a singular waveguide. *Mon. Wea. Rev.*, **107,** 751–774.

van Loon, H., R. L. Jenne, and K. Labitzke, 1973: Zonal harmonic standing waves. *J. Geophys. Res.*, **78,** 4463–4471.